JOURNAL OF AGRICULTURAL AND FOOD CHEMISTRY

Studies on Proofing of Yeasted Bread Dough Using Near- and Mid-Infrared Spectroscopy

NICOLETTA SINELLI,[†] ERNESTINA CASIRAGHI,*[,†] AND GERARD DOWNEY[‡]

Department of Food Science and Technologies, University of Milan, Via Celoria 2, 20133 Milan, Italy, and Teagasc, Ashtown Food Research Centre, Ashtown, Dublin 15, Ireland

Dough proofing is the resting period after mixing during which fermentation commences. Optimum dough proofing is important for production of high quality bread. Near- and mid-infrared spectroscopies have been used with some success to investigate macromolecular changes during dough mixing. In this work, both techniques were applied to a preliminary study of flour doughs during proofing. Spectra were collected contemporaneously by NIR (750−1100 nm) and MIR (4000–600 cm^{-1}) instruments using a fiberoptic surface interactance probe and horizontal ATR cell, respectively. Studies were performed on flours of differing baking quality; these included strong baker's flour, retail flour, and gluten-free flour. Following principal component analysis, changes in the recorded spectral signals could be followed over time. It is apparent from the results that both vibrational spectroscopic techniques can identify changes in flour doughs during proofing and that it is possible to suggest which macromolecular species are involved.

KEYWORDS: NIR spectroscopy; MIR spectroscopy; dough; proofing

INTRODUCTION

Bread is a staple dietary item in most countries of the world. Its success arises from the ability of gluten proteins to form an extensible network which may then be set during baking. Key determinants of bread quality involve flour compositional parameters (protein quality and quantity, starch damage, endogenous enzyme levels, etc.) and process variables such as mixing, proofing, and baking. Understanding the molecular changes that take place during the baking processes facilitates the development of, e.g., breads with improved quality and consistency, and considerable efforts have been made in this direction in the recent past.

The importance of mixing has long been recognized, and research efforts have led to the introduction, for example, of the Chorleywood bread process with its emphasis on reduced mixing times and the input of high energy to facilitate gluten development (*1*).

Dough proofing is also an important step during the production of good quality bread. During proofing (i.e., the resting period after mixing during which fermentation takes place) the mixed bread-making ingredients are converted, under controlled temperature, time, and humidity, to a soft and expanded dough with significant changes in both structural and rheological properties (*2*). Important aspects of the proofing stage are gas production, gas retention, and dough development (*3, 4*). During fermentation, the action of carbohydrate enzymes (α-amylase and β-amylase) converts starch to dextrins and sugars; these enzymes are present in variable amounts in wheat flour but are often added as part of an improver mixture. The action of yeast on these low molecular weight carbohydrates results in the production of carbon dioxide, which increases dough volume and contributes to overall shape and crumb texture development. Partial hydrolysis of native wheat proteins by protease enzymes, endogenous or added, softens the gluten and changes the rheological properties of dough (*5*). Dough performance is also affected by formulation, particularly by sugar, fat, and/or emulsifier addition (*6, 7*).

For the production of high-quality baked goods, the dough proofing phase needs to be optimized. Insufficient proofing times result in loaves of reduced volume and poor cell structure while excessive proofing will produce doughs of low viscosity which are difficult to handle. Overlong proofing times also represent an undue cost to the baker.

In order to produce high-quality breads efficiently, all steps in the baking process need to be optimized. Rheofermentometry (Chopin, Paris, France) is one method used to monitor proofing; in particular, this technique can provide useful information about flour and/or dough systems based on measurements of dough rise, gas formation, and gas retention. Used in conjunction with the alveograph as a mixer, the instrument is designed to test the quality of flour for French bread at a relatively low and fixed water absorption (*8, 9*). However, this method is slow, not suited to automation, requires high manual dexterity, and is only suitable for use by trained personnel.

Infrared spectroscopy in both the near-infrared (NIR) and mid-infrared (MIR) regions is probably one of the most powerful and convenient analytical tools which could be used to monitor

* To whom correspondence should be addressed. Tel: +39-02-5031-9184. Fax: +39-02-5031-9191. E-mail: ernestina.casiraghi@unimi.it.
[†] University of Milan.
[‡] Ashtown Food Research Centre.

10.1021/jf0727138 CCC: $40.75 © 2008 American Chemical Society
Published on Web 01/15/2008

dough leavening given that absorptions in these spectral ranges can be related, to a greater or lesser degree, to the principal chemical components of dough–water, protein, starch, and fat (*10–12*). While MIR measurements have advantages because they provide information on fundamental molecular vibrations (*13–15*), NIR measurements are easier to make and, owing to their higher energy content, may penetrate dough pieces to a greater distance than MIR radiation, thus potentially producing more representative measurements. NIR spectra have been used to monitor the content of sucrose, fat, flour, and water in biscuit doughs (*16, 17*) and also to investigate key macromolecular changes which occur during dough mixing (*18–22*). Due to its noninvasive nature, NIR has the potential to be used in an online monitoring system for bread manufacturers to optimize the mixing process.

In this work, both near- and mid-infrared spectroscopy were applied in a preliminary study of the proofing of bread doughs involving flours of different baking quality. Studies were also performed on gluten-free flours which lack the ability to form elastic doughs due to the absence of gluten protein (*23*). Both spectroscopic techniques were used to investigate macromolecular changes during the proof phase with the aims of characterizing any such changes and determining optimum proofing times based on objective spectral readings rather than acquired bakery experience.

MATERIALS AND METHODS

Dough Preparation. Three different types of commercial flours (Odlum Group Ltd., Dublin, Ireland) were used in this study. These were (a) strong baker's flour comprising wheat flour, vital wheat gluten, calcium carbonate, and α-amylase with a protein content of 11–12% (at 14% moisture), (b) retail or soft flour comprising wheat flour and raising agents (sodium bicarbonate, monocalcium phosphate, sodium acid pyrophosphate) with a protein content of 8–9% (at 14% moisture), and (c) gluten-free flour comprising wheat starch, soya flour, modified maize starch, raising agents (calcium acid phosphate, sodium bicarbonate) salt, calcium carbonate, stabilizer (methylhydroxypropyl and cellulose), vitamins (B1, B2; niacin), and iron with a protein content of 4.6% (at 14% moisture). The presence of raising agents and acid in some of these formulations is a confounding factor, but these recipes are typical commercial formulations used in Ireland, and the goal of this exploratory work was to monitor molecular modifications occurring during proofing as occurring industrially.

The standard recipe for bread production using strong baker's flour was as follows: flour (1000 g), water (615 g), yeast (28 g), and sodium chloride (20 g). Using retail flour, this recipe was modified by using a reduced quantity of water (550 g). For both recipes, water (at 30 °C), flour, and yeast were placed into the mixing bowl of a domestic mixer (Chef, Kenwood, U.K.) fitted with a dough mixing attachment and mixed for a total of 10 min. The recipe for gluten-free dough was as follows: gluten-free flour (1000 g), water at 35 °C (870 g), and fresh yeast (28 g). Ingredients were mixed for a total of 4 min in a three-speed mixer (Model A120, Hobart, U.K.). All experiments, including dough mixing and proofing, were carried out twice.

NIR Spectroscopy. NIR spectra were collected by a NIRSystems 6500 scanning monochromator (FOSS NIRSystems, Silver Springs, MD) fitted with a fiberoptic surface interactance probe over the range 750–1100 at 2 nm intervals. This wavelength range was chosen because of the greater radiation depth associated with it as compared to the longer, conventional NIR range (1100–2498 nm). For each test, spectra were collected directly from the dough surface every 2 min during proofing periods of up to 1 h and stored as $\log(1/R)$; once positioned, the interactance probe was not moved during the 1 h proofing period. During testing, doughs were placed in a baking tin which was maintained at 30 °C in a water bath; dough temperature was monitored using a digital thermometer (Eirelec, MT 130 TC; Technology House, Dundalk, Ireland) while the baking tin was covered with cling film to prevent moisture loss from the dough. WinISI software (v.1.04a; FOSS NIRSystems, Silver Springs, MD) was used for spectral acquisition, instrument control, and preliminary file manipulation.

MIR Spectroscopy. FT-IR measurements were taken using a spectrometer (Bio-Rad Excalibur series FTS 300; Analytica Ltd., Dublin, Ireland) equipped with a deuterated triglycine sulfate (DTGS) detector. Win-IR-Pro software (v.3.0, Bio-Rad; Analytica Ltd., Dublin, Ireland) was used for spectral acquisition, instrument control, and preliminary file manipulation. Spectra were recorded using an in-compartment benchmark attenuated total reflectance (ATR) trough top plate by use of a 45° Ge crystal with 11 internal reflections. For both background and sample readings, 64 scans were coadded at a nominal resolution of 8 cm^{-1}; single beam spectra of the samples were collected and ratioed against a background of air. Freshly prepared dough samples were positioned on the ATR plate with great care so as to minimize stress and shear forces. For each test, spectral data were collected in the range 4000–600 cm^{-1} at room temperature (20 ± 0.5 °C) every 2 min during proofing periods of up to 1 h; after initial placement, dough samples were left undisturbed during the entire 1 h testing period. While samples were not directly covered during these spectral collection periods, the lid of the sample compartment was kept closed throughout. A feature around 2300 cm^{-1} in the FTIR spectra was an aberration due to the presence of atmospheric CO_2 in the ATR sample compartment; for this reason, spectral data between 2280 and 2420 cm^{-1} were removed prior to data analysis.

Data Processing. Both NIR and MIR spectral data sets were analyzed using The Unscrambler (version 9.7; Camo, Trondheim, Norway) software. NIR spectral data were pretreated using a second derivative transform calculation (Savitzky−Golay method, gap size = 10 data points). Principal component analysis (PCA) was applied as an exploratory tool to both NIR and MIR spectral data to detect unusual or outlying samples and to uncover spectral trends occurring during the proof phase. PCA identifies orthogonal directions of maximum variance in the original data set in decreasing order and projects the data onto a lower dimensionality space formed by a subset of the highest variance components. The orthogonal directions are linear combinations of the original variables, and each component explains in turn a part of the total variance of the data; in particular, the first significant component explains the largest percentage of the total variance, the second one, the second largest percentage, and so forth (*24, 25*). All spectra collected during the proofing were averaged to produce a single spectrum for each dough type and proofing time. All spectral data sets were mean-centered before performing PCA calculations. The mean values of the PC scores were then modeled as a function of time to identify critical points during proofing (Table Curve Software, v.4.0; Jandel Scientific, San Rafael, CA).

Analysis of variance of proofing critical point values was performed by using the statistical software SYSTAT (version 5.03, Systat 5.03 for Windows; Systat Inc., Evanston, IL), applying the Tukey test.

RESULTS

NIR Spectroscopy. Reflectance spectra of a strong baker's flour dough collected over a 1 h proofing period are shown in **Figure 1**. Raw spectra reveal few defined features except for a peak at 982 nm although there are also some suggestions of spectral undulations centered around 750 and 840 nm. The major feature of this spectral collection, however, is a vertical offset of the spectra with the recorded absorbance values increasing during the first 6 min and then consistently decreasing with increasing proof time; the magnitude of the offset varies with proofing time as indicated by the gaps between spectra in **Figure 1**. Absorbance changes during each 2 min sampling period are lowest at the beginning and end of the proofing time studied. The overall effect appears to be wavelength independent over the range scanned. Such a linear offset may indicate some systematic change in composition of the dough matrix, altered penetration distance of radiation into the dough, or perhaps a reduction in dough density during proofing time. All three

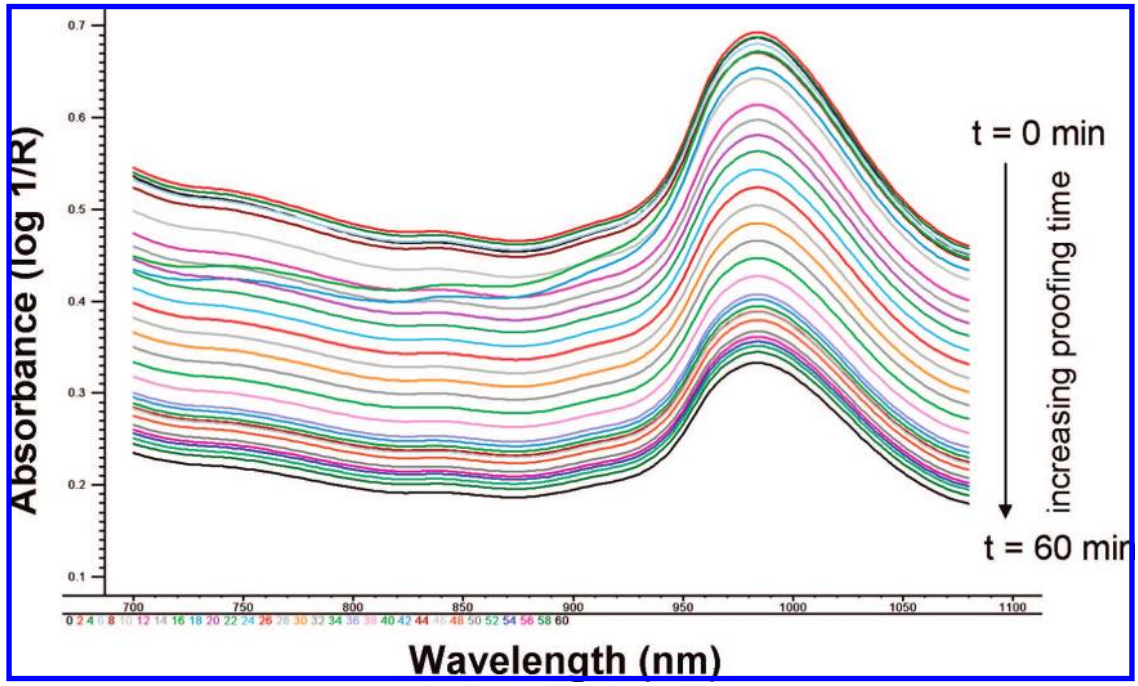

Figure 1. Reflectance spectra of a strong baker's flour dough collected over a 1 h proofing period.

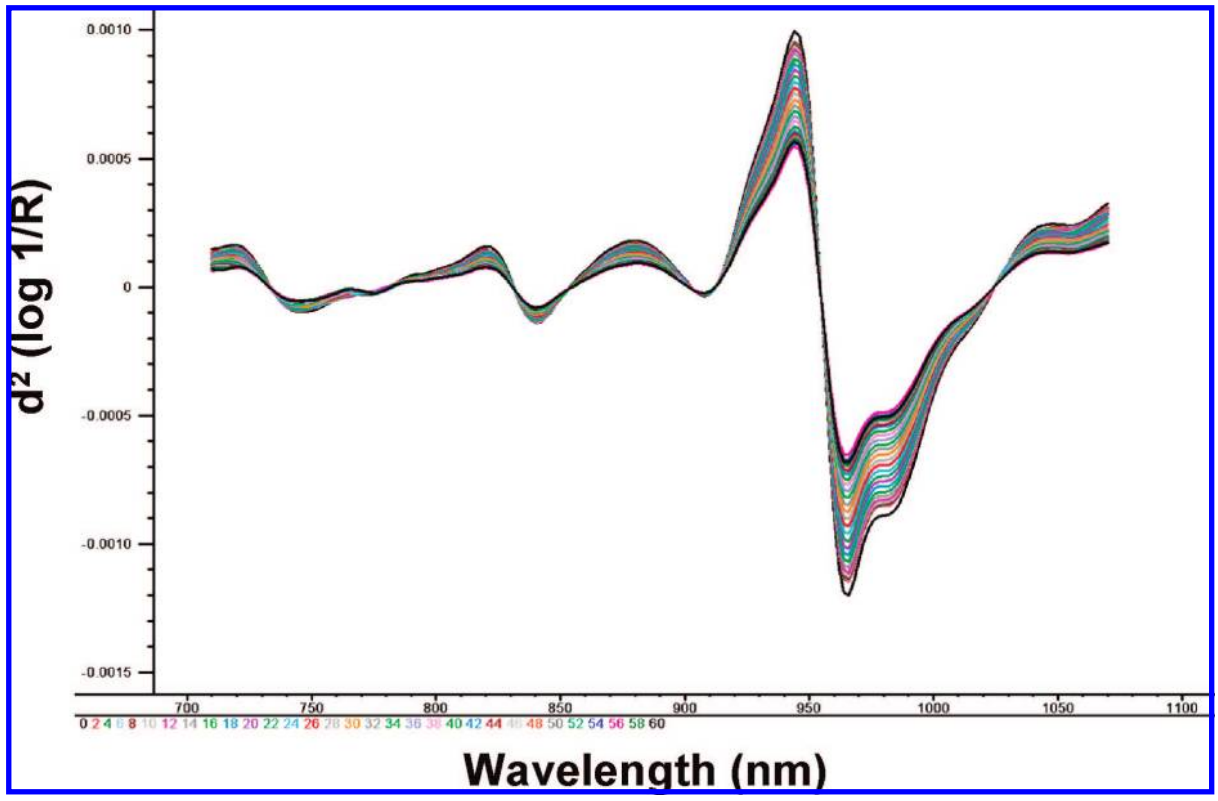

Figure 2. Second derivative reflectance spectra of a strong baker's flour dough collected over a 1 h proofing period.

possibilities are in agreement with the known events taking place in a dough during proof. After a second derivative treatment, several spectral features become more apparent (**Figure 2**). These comprised troughs at approximately 740, 840, and 960 nm with a shoulder centered at 982 nm; minima in this second derivative plot correspond to maxima in the raw spectral data. Absorbance at all of these wavelengths has been attributed to water: third overtone –OH stretch (740 nm), −OH combination band (840 nm), second overtone –OH stretch (970 nm), second overtone –OH hydrogen-bonded to other species such as sugars or starch (980 nm) (*26*). At this point, it is therefore possible to state that NIR spectra recorded in this wavelength range are able to detect some changes which occur during dough proofing.

PCA was performed on the second derivative NIR spectra collected during dough proofing, and the sample scores calculated on PCs 1 and 2 were plotted, together with the loading plots of the first three principal components in **Figures 3**−**5** for strong baker's, retail, and gluten-free flour, respectively. On score plots the number beside each point represents the proofing

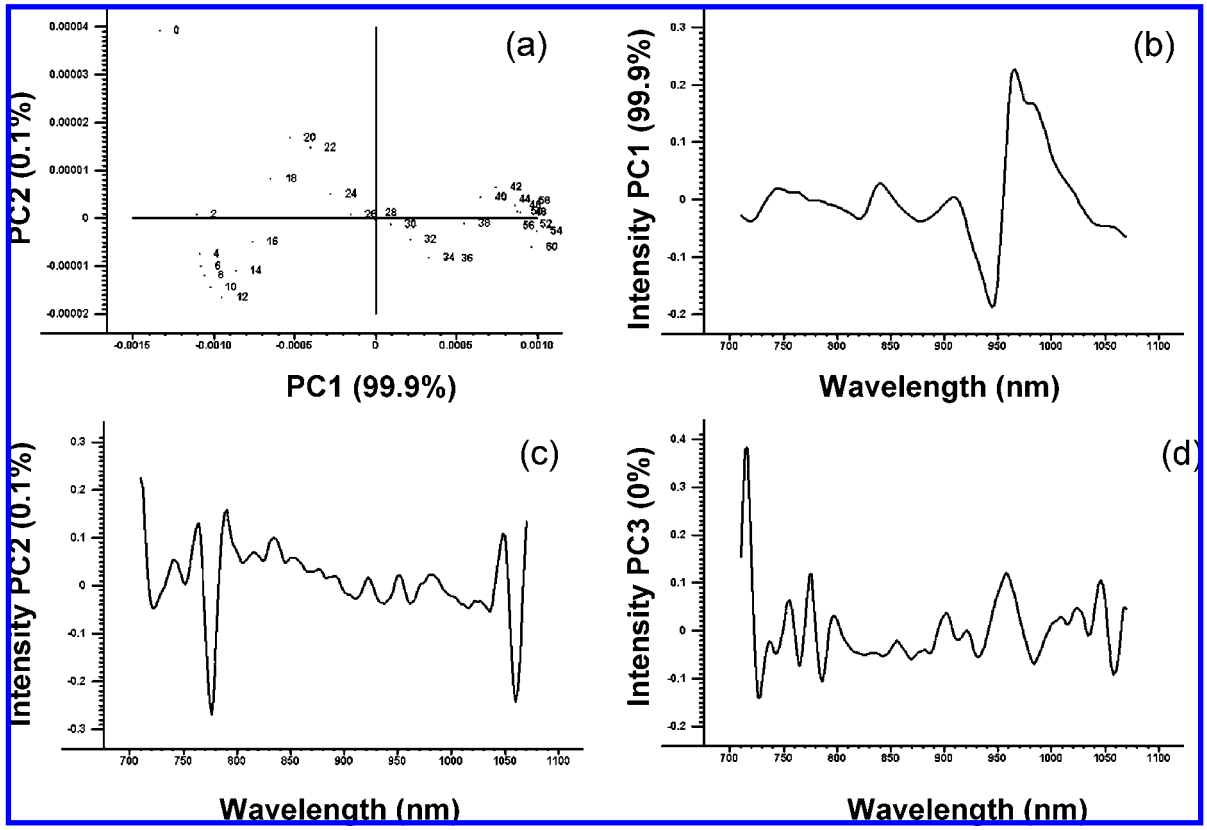

Figure 3. Principal component scores (**a**) and loading plot PC1 (**b**); PC2 (**c**) and PC3 (**d**); NIR spectra of strong baker's flour during proofing.

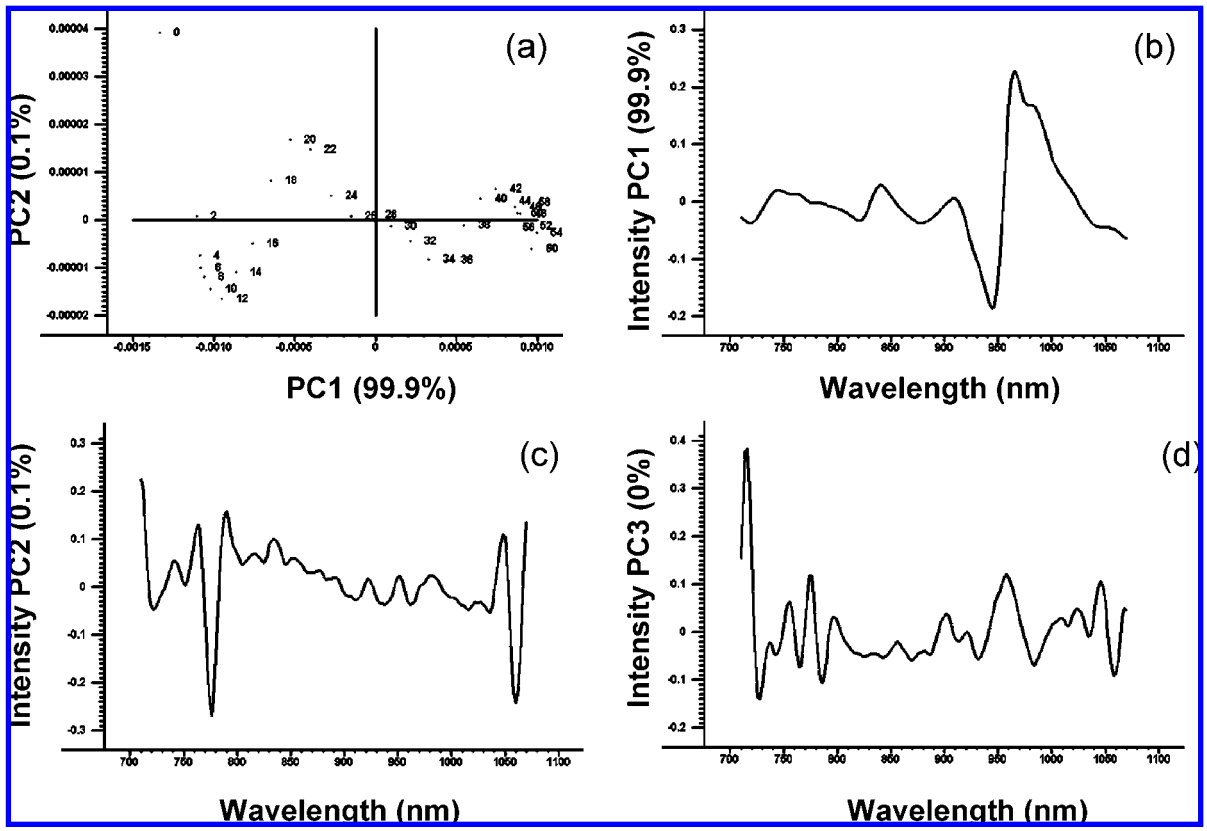

Figure 4. Principal component scores (**a**) and loading plot PC1 (**b**); PC2 (**c**) and PC3 (**d**); NIR spectra of retail flour during proofing.

time in minutes. In the case of strong baker's flour a number of significant features are evident in **Figure 3a**. First, samples are distributed along PC1, which accounts for 99.9% of the variance in the spectral collection, from left to right mainly on the basis of increasing proofing time. This distribution is especially clear up to a time of 44 min but becomes less clear thereafter. Superimposed on this distribution is a complex behavior on PC2 which, although it only accounts for approximately 0.1% of

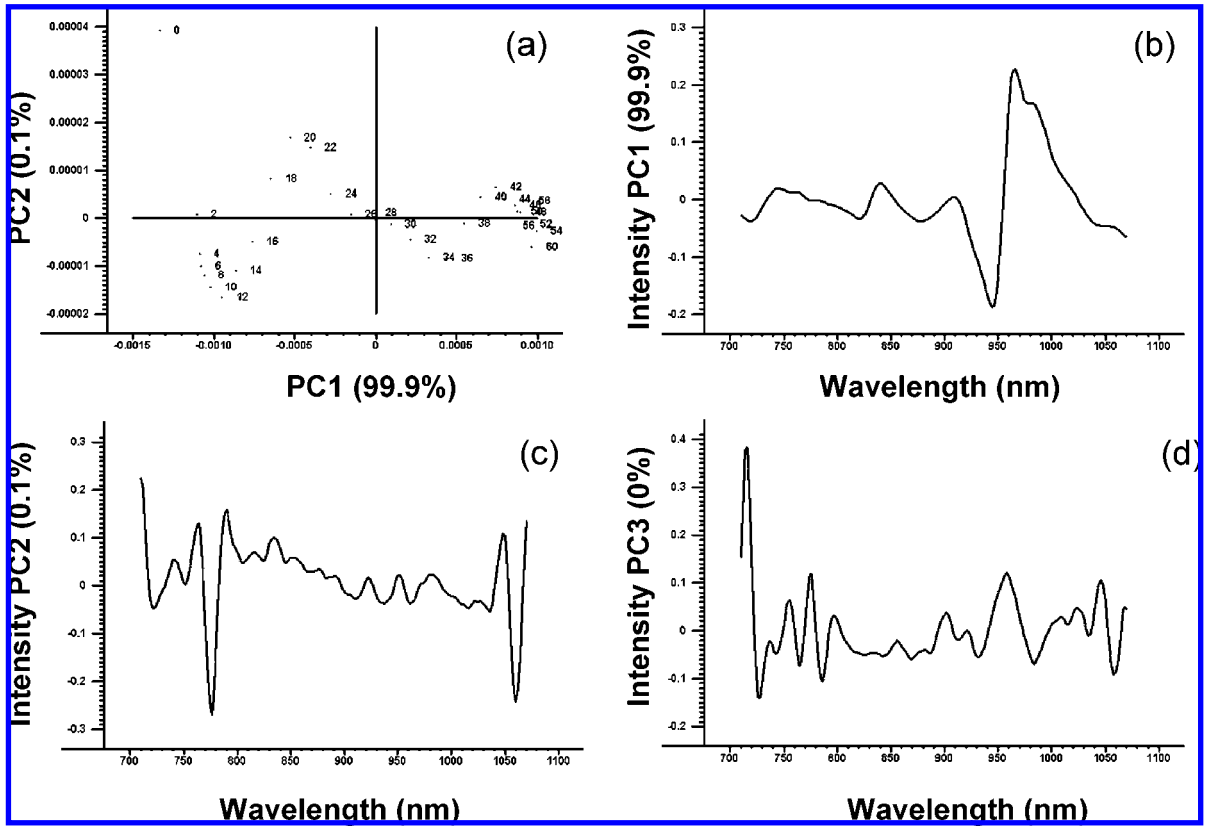

Figure 5. Principal component scores (**a**) and loading plot PC1 (**b**); PC2 (**c**) and PC3 (**d**); NIR spectra of gluten-free flour during proofing.

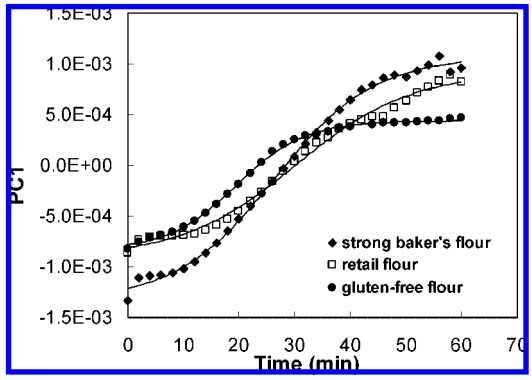

Figure 6. PC1 scores versus time for strong baker's, retail, and gluten-free flour during proofing.

Table 1. Maximum Acceleration (max d^2x/dt^2), Maximum Rate (max dx/dt), and Maximum Deceleration (min d^2x/dt^2) Time of Spectral Change during Proofing for the Three Flour Types[a]

type of dough	max d^2x/dt^2 (min)[b]	max dx/dt (min)[c]	min d^2x/dt^2 (min)[d]
strong baker's flour	14.61 ± 1.92a	26.40 ± 0.86b	38.18 ± 1.60b
retail flour	16.61 ± 2.40a	30.29 ± 0.44b	43.97 ± 2.35b
gluten-free flour	11.38 ± 2.55a	19.51 ± 3.83a	27.65 ± 5.86a

[a] Mean values bearing the same letters are not significantly different ($p > 0.05$). [b] Max d^2x/dt^2 = maximum of the second derivative. [c] Max dx/dt = maximum of the first derivative. [d] Min d^2x/dt^2 = minimum of the second derivative.

spectral variance, results in an almost sinusoidal pattern of sample score distribution.

In an attempt to uncover the causes of these score patterns, each principal component was studied. Examining the loadings of PC1 (**Figure 3b**), a number of significant features may be identified: a minimum at 944–946 nm, which corresponds to the first overtone of O−H symmetric and asymmetric stretching in water molecules, and a shoulder at 978−984 nm, which has been attributed to the first overtone of O−H symmetric or C−H of starch. Molecular events related to the features at 966–968 and 978–984 nm are opposed to those responsible for the feature at 944–946 nm and account for the distribution of spectra from left to right along PC1. This principal component closely resembles an inverted mean second derivative spectrum; this is to be expected given the observation above that the main feature of the raw spectra was an offset with time. It is not possible to explain the score behavior on PC2 at this time nor is any satisfactory interpretation of PC2 possible (**Figure 3c**) with the main features of this principal component occurring in the visible wavelength region (<780 nm) and at 1060 nm. This component accounted for <0.1% of variance in the original spectral data set. Thus we can state that NIR spectroscopy is tracking molecular events involving water and starch as the main source of spectral variance during this dough proofing experiment.

Both replicates for doughs produced from the other flour types (i.e., retail and gluten-free) were treated as described above and exhibited similar behavior, different from those of strong baker's flour. The corresponding score and loading plots are shown in **Figures 4** and **5**. In both cases, samples appear distributed from left (proofing starting time) to right (proofing end time) along the first component, which accounts for 99.9% of the total variance in the spectral data set. It is interesting to observe that retail dough and gluten-free dough do not differ significantly from each other. In this case also, the proofing phenomena relate to water and starch absorption bands.

To better describe the spectral changes undergone during proofing by each type of dough, the relevant PC1 scores were

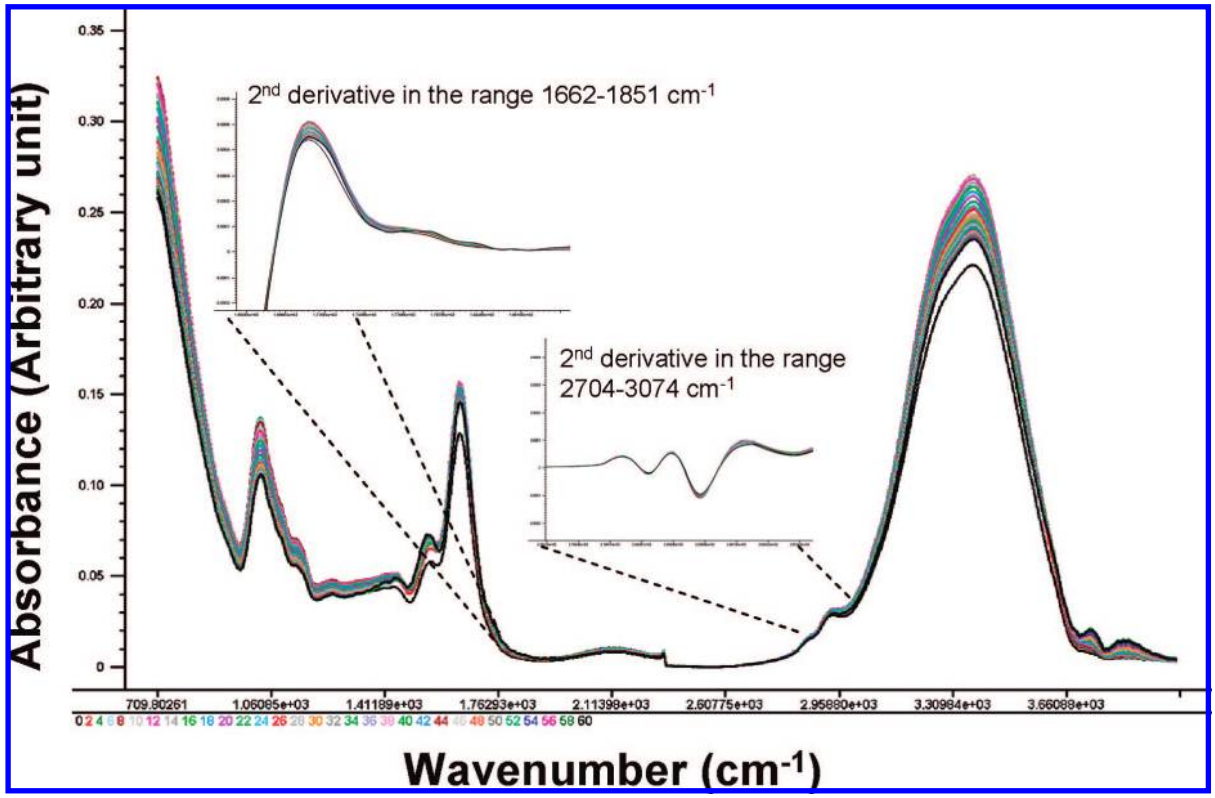

Figure 7. ATR spectra of a strong baker's flour dough collected over a 1 h proofing period with higher resolution plots of second derivative peaks in the 2704–3074 and 1662−1851 cm^{-1} regions.

plotted against time (**Figure 6**) and modeled using a sigmoid function expressed as

$$y = a + b/[1 + \exp(c - x)/d]$$

where a is the maximum shift (from initial to equilibrium value) of the considered index, b is the transition center, t is the proofing time, and c and d are two constants. All experimental data were well-fitted ($r^2 > 0.98$) by this sigmoid function. In fact, the use of this type of function is justified by the nature of the transformations in progress. Yeast is stored at low temperature (4 °C) prior to use in order to minimize enzyme activity in the yeast block. When mixed with the other ingredients in dough, it exhibits low metabolic activity and begins the fermentation of naturally occurring sugars (glucose and sucrose) in the flour, breaking them down into ethanol and CO_2; as metabolic activity increases, yeast enzymes begin the breakdown of damaged starch into dextrins and maltose which later then acts as a fermentation substrate to produce high rates of CO_2 evolution. Eventually, gas production rates slow as available substrate decreases. Such behavior is accurately described by a sigmoid curve which starts with a lag phase, increases to an inflection point, and finally slows to approach asymptotically a constant value (*27, 28*).

For each of the three flour types the maximum of the first derivative and maximum and minimum of second derivative are shown in **Table 1**. In the case of strong baker's and retail flour doughs, the maximum rate of spectral change (maximum of the first derivative) occurred at about 26 and 30 min, respectively. The time at which the acceleration of the process was maximal for these two flour types was about 15 (strong baker's) and 17 min (retail), respectively. This time, corresponding to the maximum of the second derivative, is associated with the first phase of the proofing. The time at which deceleration of the process was greatest, corresponding to the minimum of the second derivative, was at about 38 and 44 min for strong baker's and retail dough, respectively; this event can be associated with the end of the proof phase (*29, 30*).

The time at which these key parameters occurred in the case of gluten-free flour doughs was shorter than the others although the maximum acceleration time was statistically not significantly shorter ($p < 0.05$); this is shown by the plot of gluten-free dough in **Figure 6**. It may be the case that the processes being followed spectrally occur quicker in the gluten-free flour on account of the greater diffusion of CO_2 to the atmosphere given the absence of an extended, strong gluten network to effect significant retention (*23*). Although retail flour is characterized by weaker protein quality, usually associated with the formation of fewer, larger gas bubbles, no statistical differences are evident between strong baker's and retail flour dough.

MIR Spectroscopy. An example of the ATR Fourier transform infrared (FTIR) spectra of strong baker's dough collected during proofing for 1 h is shown in **Figure 7**. The spectra are dominated by peaks attributed mostly to water (3379 cm^{-1}), carbonyl stretching of gluten protein (amide I) in combination with the OH deformation of water (1647 cm^{-1}), NH bend and CN stretch of gluten protein (amide II) at 1543 and 1554 cm^{-1}, and the coupled C−O and C−C stretching vibrations of starch at 1023, 1080, and 1153 cm^{-1}. Small features due to the presence of carbonyl groups in the dough are present at 2963, 2928, and 2854 cm^{-1} (C−H stretch of CH_2 and CH_3) and a shoulder centered around 1740 cm^{-1} (carbonyl stretch of the fat triglyceride ester linkage) (*31, 32*). These peaks are more evident in the second derivative of the spectra; higher resolution plots of these regions is shown in **Figure 7**.

For each type of dough, PCA was performed on the raw spectral data in the range 4000−710 cm^{-1}. In the case of strong baker's flour dough, the distribution of sample scores on PCs 1

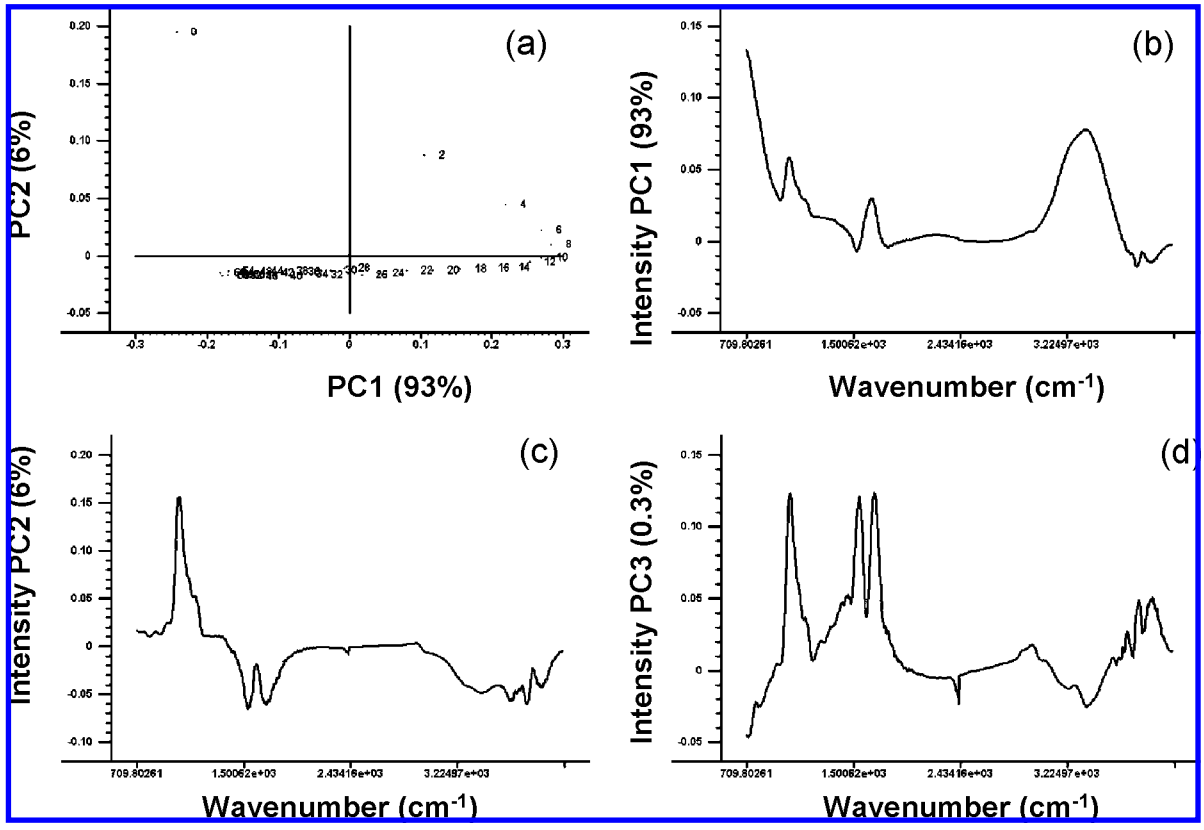

Figure 8. Principal component scores (**a**) and loading plot PC1(**b**); PC2 (**c**) and PC3 (**d**); FTIR spectra of strong baker's flour during proofing.

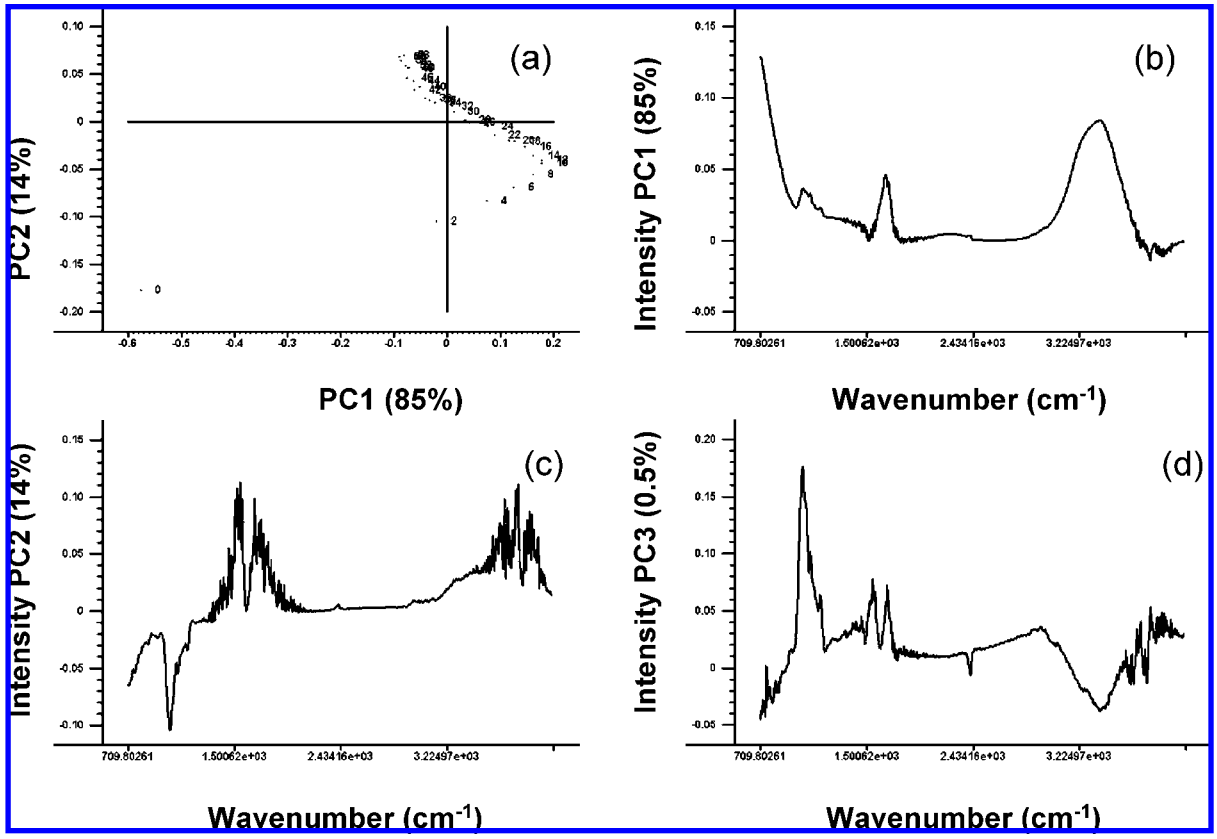

Figure 9. Principal component scores (**a**) and loading plot PC1 (**b**); PC2 (**c**) and PC3 (**d**); FTIR spectra of retail flour during proofing.

+ 2 describes a complicated relationship with proofing time as shown in **Figure 8a**. The main feature of this plot is a distribution of spectra along PC1, which accounted for 93% of the total variance in the spectral data set, in two directions and involving a directional change at around 10 min. PC2, accounting for 6% of total spectral variance, effected a separation of spectra collected at 2, 4, 6, and 8 min from the others; this behavior was quite different from that observed in the case of

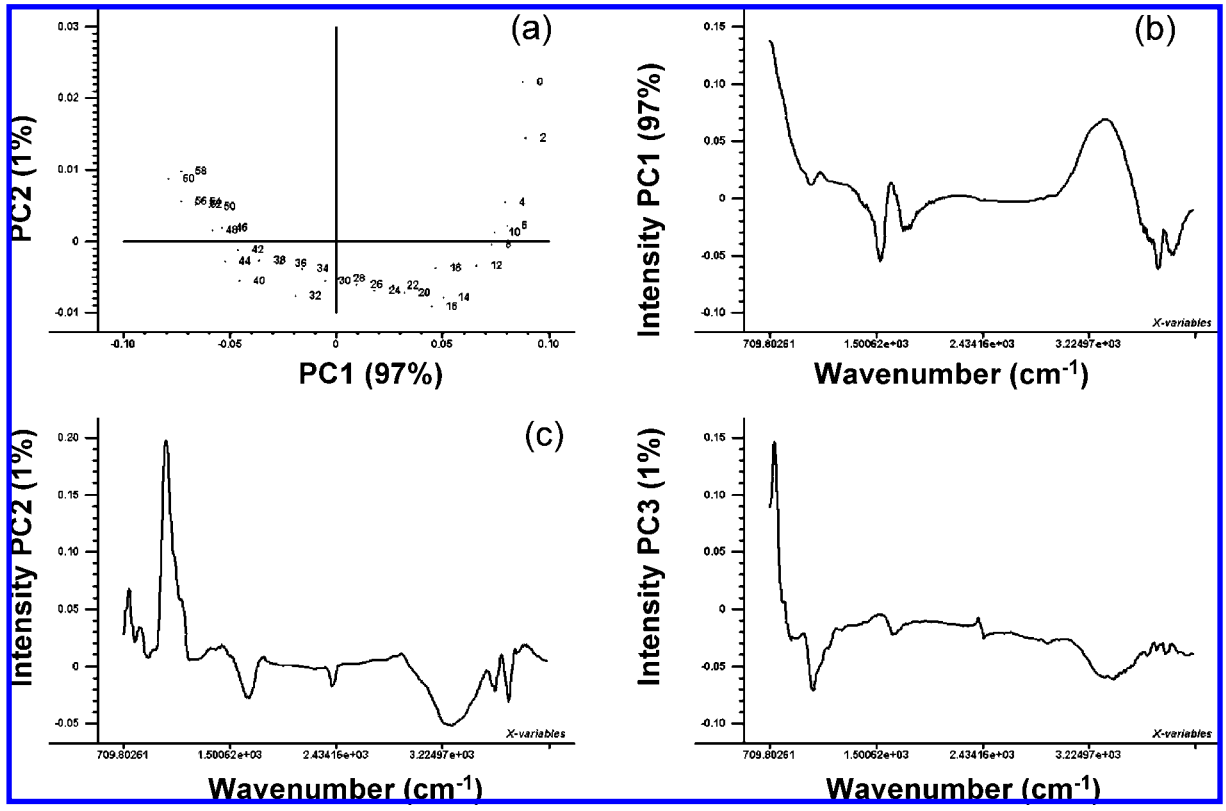

Figure 10. Principal component scores (**a**) and loading plot PC1 (**b**); PC2 (**c**) and PC3 (**d**); FTIR spectra of gluten-free flour during proofing.

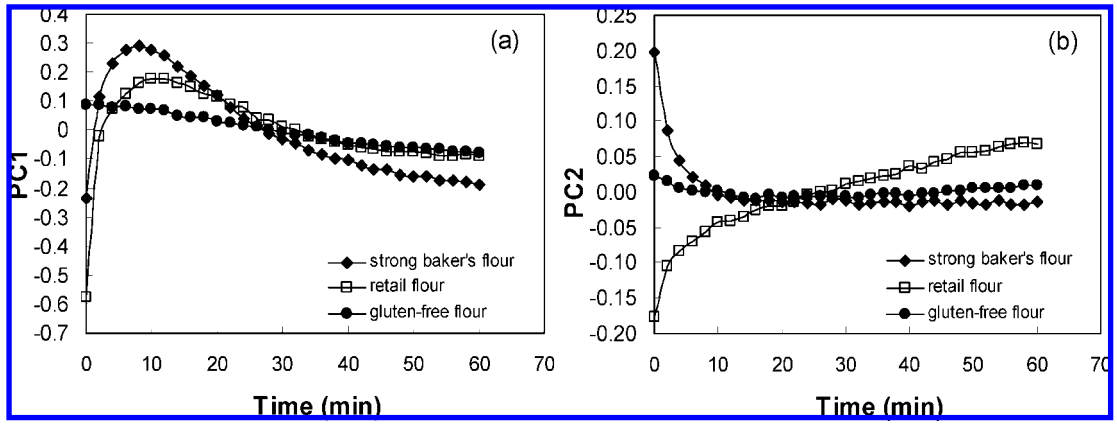

Figure 11. PC1 (**a**) and PC2 (**b**) scores versus time for strong baker's, retail, and gluten-free flour during proofing.

NIR spectra (**Figure 3**). Principal component 1 (**Figure 8b**) was characterized by positive contributions from water (3375 cm^{-1}), starch (maxima at 1022, 1080, and 1150 cm^{-1}), and protein (amide I, 1632 cm^{-1}); the relative importance of these components was different from those in the original spectra with absorptions due to water and starch being approximately equal in magnitude and larger than those arising from protein bands. Interestingly, absorbances arising from the amide II groups which were present in the original spectra were not significant in this principal component. The presence of fat was reflected in a small shoulder centered around 2959 cm^{-1}. In the case of PC2 (**Figure 8c**), starch absorptions were positive and largest in magnitude; these were in opposition to minima at 1539 and 1651 cm^{-1} (which may be ascribed to amide II and amide I bands in protein, respectively) and water (*28, 29*). PC3 (**Figure 8d**) accounts for less than 1% of the total variability in the sample data set but does influence the distribution of sample scores in a U-shape with time, suggesting the occurrence of a process which reverses. Examination of PC3 reveals the most important molecular species to be associated with the amide I and amide II protein bands (maxima at 1651 and 1543 cm^{-1}); starch absorptions are present at slightly lower intensities. Small peaks are detectable at 1246 and 1317 cm^{-1}; absorptions at these frequencies have been attributed to β-sheet and α-helical conformations of gluten proteins (*33*), but given their magnitude in this plot and the degree of noise present, it is not possible to be unequivocal about their importance.

Retail flour exhibits behavior which closely resembles that of strong baker's flour, i.e., a distribution of sample scores in one direction along PC1 until t = 8–10 min followed by a direction reversal (**Figure 9a**). Plots of the principal components were very similar to those of baker's flour although the relative size of the major features differed somewhat. For example, in the case of PC1 (**Figure 9b**), the relative importance of starch and protein absorptions by retail flour is reversed from the baker's flour situation. Gluten-free doughs exhibited behavior which was quite different with regard to the sample score distribution; in this case, distribution along PC1 was on the basis

of time of proofing and the observed direction reversal was on PC2, with the change point occurring at around $t = 16$ min (**Figure 10a**). With regard to the principal component graphs, the major features in PC1 were water and protein (amide II; 1539 cm^{-1}); in this component, small unattributed absorptions were present at 1003, 1045, and 1070 cm^{-1}. A positive contribution by starch was the main feature in PC2, in opposition to protein (amide I; 1632 cm^{-1}) and water absorbances; an unattributed minimum at 2272 cm^{-1} was also present, which was approximately equal in magnitude to the protein absorbance minimum.

As was the case for NIR spectra, the PC1 FTIR scores were plotted against time (**Figure 11**). Examination of **Figure 11a** reveals that doughs produced from strong baker's and retail flour exhibit an increase in PC1 score value up to 8 min (strong baker's) and 12 min (retail) after mixing, respectively; after this maximum value has been reached, scores decrease to reach a plateau minimum after about 50 min in both cases. In the case of PC2 scores (**Figure 11b**), the behavior of strong baker's and retail flours is in opposition; scores for strong baker's flour doughs decrease from a maximum at $t = 0$ and level off from around $t = 20$ min; for retail flour doughs, PC2 scores increase rapidly from a minimum at $t = 0$ until around $t = 10$ min and then gradually through the remainder of the proofing time. In contrast to these behaviors, gluten-free flour doughs exhibit a slow decline in score values on PC1 and a similar decline on PC2 up to about 15 min, after which they level off over the complete time course of the experiment. It is apparent from a comparison of **Figures 6** and **11** that the recorded behavior of the doughs in the NIR and MIR spectral regions is different. The exact cause of this difference is unclear but may arise in part from the different penetration depths of the respective radiation into dough samples.

DISCUSSION

It is apparent from the preceding results that both vibrational spectroscopic techniques can identify changes in flour doughs during proofing and that it is possible to suggest which macromolecular species are involved. However, certain differences between the techniques are discernible. NIR data suggest that (1) the main species involved during proofing relate to water and starch and (2) doughs made from gluten-free flour behave in much the same way as the other two types. FTIR data collected on the doughs made from the same flour types paint a more detailed and nuanced picture; in particular, while the relative role of starch and water are as for the NIR data, principal component analysis reveals a greater role for protein during this dough development stage. With regard to gluten-free flour doughs, FTIR data indicate behavior which contrasts with that of the NIR data set. The main macromolecular species accounting for dough changes during proofing was protein while starch was of secondary importance and only present in PC2. However, a note of caution must be sounded regarding this comparison. While the NIR spectral data may be considered a good approximation of bulk dough properties given the likely penetration distance into the sample, the ATR presentation used for collection of FTIR spectra only interacts with the sample doughs to a distance which is measured in microns. This latter sampling technique therefore is restricted essentially to the observation of phenomena on the dough surface.

A potential commercial exploitation of this approach could involve the prediction of the optimum proofing time for any given flour dough using, for example, the time of maximum deceleration of the spectral change process. That the time obtained for strong baker's flour to reach this point in the work reported in this paper (approximately 38 min) is slightly shorter than the normal proofing time used for the Chorleywood bread process (50 min) suggests that a reevaluation of this time may be merited.

LITERATURE CITED

(1) Zhou, W.; Therdthai, N. Manufacture. In *Bakery Products Science and Technology*, 1st ed.; Hui, Y. H., Ed.; Blachwell Publishing: Ames, IA, 2006; pp 301–317.
(2) Abdelrahman, A.; Spies, R. Dynamic rheological studies of dough systems. In *Foundamentals of Dough Rheology*; Faridi, H., Faubion, J. M., Eds.; American Association of Cereal Chemists: St. Paul, MN, 1986; pp 87–103.
(3) Yang, C.-H. Fermentation. In *Bakery Products Science and Technology*, 1st ed.; Hui, Y. H., Ed.; Blachwell Publishing: Ames, IA, 2006; pp 261–271.
(4) Dobraszczyk, B. J.; Campbell, G. M.; Gan, Z. Bread: an unique food. In *Cereals and Cereal Products. Chemistry and Technology*; Dendy, D. A., Dobraszczyk, B. J., Eds.; Aspen Publishers: Gaithersburg, MD, 2001; pp 182–232.
(5) De Leyn, I. Functional Additives. In *Bakery Products Science and Technology*, 1st ed.; Hui, Y. H., Ed.; Blachwell Publishing: Ames, IA, 2006; pp 233–259.
(6) Dobraszczyk, B. J. Measuring the rheological properties of dough. In *Bread making, Improving quality*; Cauvin, S. P., Ed.; CRC Press: Boca Raton, FL, 2000; pp 375–400.
(7) Dobraszczyk, B. J. Wheat and Flour. In *Cereals and Cereal Products, Chemistry and Technology*; Dendy, D. A. V., Dobraszczyk, B. J., Eds.; Aspen Publishers: Gaithersburg, MD, 2001; pp 100–139.
(8) Czuchajowska, Z.; Pomeranz, Y. Gas formation and gas retention. I. The system and methodology. *Cereal Food World* **1993**, *38*, 499–503.
(9) Hruskova, D.; Kucerova, I. The use of fermentograph for yeasted dough quality evaluation. *Getreide, Mehl Brot.* **2003**, *57*, 85–89.
(10) Cen, H.; He, Y. Theory and application of near infrared reflectance spectroscopy in determination of food quality. *Trends Food Sci. Technol.* **2007**, *18*, 72–83.
(11) Ozaki, Y.; McClure, W. F.; Christy, A. A. *Near Infrared Spectroscopy in Food Science and Technology*, 1st ed.; John Wiley and Sons: Hoboken, NJ, 2006; 408 pp.
(12) Williams, P.; Norris, K. *Near Infrared Technology in the Agricultural and Food Industries*, 2nd ed.; American Association of Cereal Chemists: St. Paul, MN, 2001; 296 pp.
(13) Colthup, N. B.; Daly, L. H.; Wiberly, S. E. *Introduction to Infrared and Raman Spectroscopy*, 3rd ed.; Academic Press: New York, 1990; 545 pp.
(14) Coates, J. Interpretation of Infrared Spectra, A Pratical Approach. In *Encyclopaedia of Analytical Chemistry*; Meyers, R. A., Ed.; John Wiley and Sons: Chichester, U.K., 2000; pp 10815–10837.
(15) Workman, J. Review of Interpretive Spectroscopy for Raman and Infrared. In *Handbook of Organic Compounds*; Workman, J., Ed.; Academic Press: London, 2001; pp 209–242.
(16) Osborne, B. G.; Fearn, T.; Miller, A. R.; Douglas, S. Application of near infrared spectroscopy to the compositional analysis of biscuits and biscuits dough. *J. Sci. Food Agric.* **1984**, *35*, 99–105.
(17) Osborne, B. G. Near infrared spectroscopic studies of starch and water in some processed cereal foods. *J. Near Infrared Spectrosc.* **1996**, *4*, 195–200.
(18) Wesley, I. J.; Larsen, N.; Osborne, B. G.; Skerritt, J. H. Non-invasive monitoring of dough mixing by near infrared spectroscopy. *J. Cereal Sci.* **1998**, *27*, 61–69.
(19) Psotka, J. Utilizing predictive technologies in milling and baking. *Cereal Food World* **1999**, *44*, 30–31.
(20) Alava, J. M.; Millar, S. J.; Salmon, S. E. The Determination of Wheat Breadmaking Performance and Bread Dough Mixing Time by NIR Spectroscopy for High Speed Mixers. *J. Cereal Sci.* **2001**, *33*, 71–81.

(21) Welsey, I. J.; Larsen, N.; Osborne, B. G.; Skerritt, J. H. Monitoring of dough properties. U.S. Patent 6,342,259 B1. 2002.
(22) Ait Kaddour, A.; Barron, C.; Morel, M.-H.; Cuq, B. Dynamic monitoring of dough mixing using near-infrared spectroscopy: physical and chemical outcomes. *Cereal Chem.* **2007**, *84*, 70–79.
(23) Gellagher, E.; Gormely, T. R.; Arendt, E. K. Crust and crumb characteristics of gluten free breads. *J. Food Eng.* **2003**, *56*, 153–161.
(24) Beebe, K. R.; Pell, R. J.; Seasholtz, M. B. *Chemometrics, a practical guide*; John Wiley and Sons: New York, 1998; 360 pp.
(25) Naes, T.; Isaksson, T.; Fearn, T.; Davies, A. M. C. *A User-Friendly Guide to Multivariate Calibration and Classification*; NIR Publications: Chichester, U.K., 2000; 344 pp.
(26) Golic, M.; Walsh, K.; Lawson, P. Short-wavelength near-infrared spectra of sucrose, glucose and fructose with respect to sugar concentration and temperature. *Appl. Spectrosc.* **2003**, *57*, 139–145.
(27) Romano, A.; Toraldo, G.; Cavalla, S.; Masi, P. Description of leavening of bread dough with mathematical modelling. *J. Food Eng.* **2007**, *83*, 142–148.
(28) Chiotellis, E.; Campbell, G. M. Proving of bread dough. I. Modelling the evolution of the bubble size distribution. *Food Bioprod. Process.* **2003**, *81*, 194–206.
(29) Benedetti, S.; Sinelli, N.; Buratti, S.; Riva, M. Shelf Life of Cresenza Cheese as Measured by Electronic Nose. *J. Dairy Sci.* **2005**, *88*, 3044–3051.
(30) Sinelli, N.; De Dionigi, S.; Pagani, M. A.; Riva, M.; Belloni, P. Spettroscopia FT-NIR nel monitoraggio on-line di prodotti da forno: lievitazione e raffermamento. *Tec. Molitoria* **2004**, *55*, 1075–1092.
(31) Van Velzen, E. J. J.; Van Duynhoven, J. P. M.; Pudney, P.; Weegels, P. L.; Van der Maas, J. H. Factors associated with dough stickiness as sensed by attenuated total reflectance infrared spectroscopy. *Cereal Chem.* **2003**, *80*, 378–382.
(32) Li, W.; Dobraszcyk, B. J.; Dias, A.; Gill, M. M. Polymer Conformation Structure of Wheat Proteins and Gluten Subfractions Revealed by ATR-FTIR. *Cereal Chem.* **2006**, *83*, 407–410.
(33) Seabourn, B. W.; Chung, O. K.; Seib, P. A.; Mathewson, P. R. A method for monitoring the rheology and protein secondary structure of dough during mixing using FT-HATR spectroscopy. Available at http://www.scisoc.org/aacc/meeting/2003/abstracts. 2003.

Received for review September 12, 2007. Revised manuscript received November 22, 2007. Accepted November 26, 2007.

JF0727138